Viscoelastic Properties of Arborescent Polystyrene-*graft*-polyisoprene Copolymers

Steven J. Teertstra and Mario Gauthier*

Department of Chemistry, Institute for Polymer Research, University of Waterloo, Ontario, Canada N2L 3G1

Received March 24, 2006; Revised Manuscript Received October 22, 2006

ABSTRACT: Arborescent polymers are highly branched macromolecules obtained from successive grafting reactions according to a generation-based scheme. Grafting side chains onto a linear substrate randomly functionalized with coupling sites thus yields a generation zero (G0) polymer, with a comb-branched structure. Further cycles of substrate functionalization and grafting lead to arborescent polymers of generations G1, G2, etc., with a dendritic architecture. Arborescent copolymers can also be obtained when side chains with a chemical composition different from the substrate are used in the last grafting cycle. Copolymers of generations G0−G3 were thus obtained by grafting polyisoprene chains with a high *cis*-1,4-unit content onto polystyrene substrates. The dynamic mechanical behavior of the arborescent polystyrene-*graft*-polyisoprene copolymers was investigated as a function of side-chain length and generation number. The zero-shear viscosity of the copolymers was lower than for linear polyisoprenes of comparable molecular weight, but its scaling behavior as a function of molecular weight was consistent with entanglement formation. The zero-shear recoverable compliance increased with the overall molecular weight of the copolymers to reach values up to 10 times larger than for the linear analogues. Isoprene copolymers of generations G0 and G1 displayed viscous flow behavior at low shear rates, their terminal relaxation time increasing with the molecular weight of the side chains. A relaxation at intermediate frequencies, associated with the polyisoprene chains, appeared at similar frequencies for copolymers of different generations with side chains of comparable molecular weights. The frequency dependence of the modulus observed for highly branched (G2 and G3) isoprene copolymers was analogous to microgels and filled polymer systems, the modulus−frequency master curves displaying thermorheological complexity with breakdown of the time−temperature superposition principle for copolymers with short side chains.

Introduction

The rheological properties of polymers depend on different factors including the composition, the molecular weight distribution, and the presence of branching. The influence of branching on the viscoelastic properties of polymers has been studied over the past several decades for a number of model systems such as star[1] and comb-branched[2] polymers. These polymers typically have a controlled architecture and a low polydispersity, allowing in-depth investigations of structure−property relations. More recently, the synthesis of dendritic polymers, a class of highly branched polymers containing multiple branching levels, has been reported in the literature. This includes dendrimers, hyperbranched polymers, and dendrigraft polymers, also known as comb-burst[3] or arborescent[4] polymers. In contrast to dendrimers and hyperbranched polymers, where branching junctions may be present at each repeat unit, dendrigaft polymers incorporate polymer segments between branching points and, consequently, have a lower branching density.[5]

Arborescent polymers are synthesized according to a "graft-upon-graft" strategy yielding branched polymers with a very high molecular weight and branching functionality in a few reaction cycles. Polymeric chains are first grafted onto a suitably funtionalized linear polymer substrate to produce a comb-branched structure, also called a generation G0 arborescent polymer. The introduction of coupling sites on the comb polymer, followed by further grafting with side chains, yields a twice-grafted or G1 arborescent polymer. Further cycles of functionalization and grafting reactions have yielded arborescent polymers of generation up to G4. Arborescent polystyrenes have been investigated extensively both in solution[6] and in the bulk state[7] to determine the influence of structure variations on the physical properties of these materials. The main conclusion from these studies is that arborescent polystyrenes act increasingly like rigid spheres as either the branching functionality is increased or the size of the arms is reduced.

In addition to homopolymers, several arborescent copolymers have been prepared by grafting polymer chains with a different composition onto polystyrene substrates.[8] The copolymers have a core−shell morphology and physical properties dominated by the polymer grafted last, due to the large proportion of the shell material in the molecule (Figure 1). The core−shell morphology of these materials was highlighted in an atomic force microscopy (AFM) imaging study of arborescent polystyrene-*graft*-polyisoprenes.[8b] These highly branched isoprene copolymers displayed interesting elastomeric properties from a qualitative viewpoint, but their rheological properties were thus far unexplored. The present investigation aims to quantify relevant viscoelastic properties for a series of well-defined arborescent polystyrene-*graft*-polyisoprenes, for comparison to a previous study on arborescent polystyrenes[7c] and other branched polymer systems.[1,2,9]

Experimental Section

Solvent and Reagent Purification. Detailed information on the purification of the solvents and reagents used in the reactions is provided as Supporting Information.

Arborescent Polystyrene-*graft*-polyisoprenes. The synthesis of arborescent graft copolymers by coupling polyisoprene chains with

* To whom correspondence should be addressed: e-mail gauthier@uwaterloo.ca.

10.1021/ma0606713 CCC: $37.00
Published on Web 02/02/2007

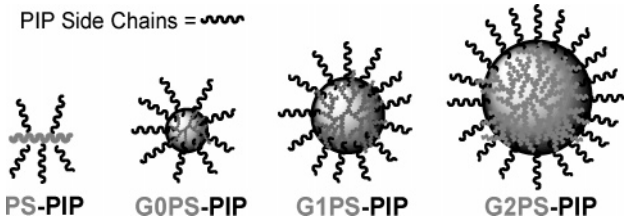

Figure 1. Hard core−soft shell morphology of arborescent polystyrene-*graft*-polyisoprenes.

polystyrene substrates bearing either chloromethyl[8b] or acetyl[10] functional groups was already reported. For this study acetyl groups were used as coupling sites, and only procedures differing significantly from those reported previously are described.

A series of linear and arborescent G0, G1, and G2 polystyrene substrates were prepared from polystyrene chains with a weight-average molecular weight $M_w \approx 5000$ and using an acetylation level of ~25 mol % at each grafting step.

Copolymers were obtained by grafting polyisoprene chains with different molecular weights onto the acetylated linear and branched polystyrene substrates. Eight copolymers with $M_w \approx 5000$, 10 000, 30 000, or 40 000 polyisoprene side chains were synthesized from the linear and G0 substrates. Four additional copolymers were produced by grafting polyisoprene chains with $M_w \approx 5000$ or 30 000 onto the G1 and G2 substrates. The polymerization of isoprene was performed in cyclohexane at room temperature to yield a microstructure with a high *cis*-1,4-units content. The preparation of a G0 copolymer from a $M_w \approx 5000$ linear polystyrene backbone and $M_w \approx 10\,000$ polyisoprene chains is provided as an example of a graft copolymer synthesis. The linear acetylated polystyrene substrate (absolute $M_w = 6500$, 1.63 g, 29% acetylation, 4.08 mequiv acetyl units) was purified in an ampule with three azeotropic distillation cycles using dry THF before redissolution in 30 mL of the solvent. A five-neck 2 L glass reactor equipped with a vacuum-tight mechanical stirrer was fitted with ampules containing purified isoprene monomer (35.2 g, 0.517 mol) and the linear acetylated substrate, dry solvent inlets from the THF and cyclohexane stills, and a septum. Solid LiCl (1.10 g, 26.0 mmol) was added to the reactor before it was evacuated, flamed, and purged with purified N_2. Cyclohexane (200 mL) was added, followed by 3−5 drops of isoprene, and the reactor was cooled to 0 °C. The solvent was titrated with *sec*-BuLi (4 drops) before the calculated amount of *sec*-BuLi initiator (2.5 mL, 3.25 mmol, for a target $M_n = 10\,000$) was added. Isoprene was added dropwise from the ampule, and the reactor was warmed to room temperature after complete addition of the monomer. The polymerization was allowed to proceed for 4 h before cooling the reactor to 0 °C and adding 350 mL of THF, thus producing a deep yellow coloration. A sample of the polyisoprene chains was removed and terminated with N_2-purged methanol. The reactor was warmed to 20 °C, and titration of the polyisoprene macroanions to a faint yellow color was performed by dropwise addition of the acetylated substrate solution. The reaction was allowed to proceed for 30 min after addition of the substrate, over which time the color faded completely. The crude product (34.7 g) was recovered by precipitation in methanol, suction filtration, and drying under vacuum. The grafting product (absolute $M_w = 157\,000$, $M_w/M_n = 1.06$, grafting yield 80%) was isolated from the linear PIP contaminant by precipitation fractionation from hexane/2-propanol mixtures. Successful fractionation was confirmed by comparison of size exclusion chromatography (SEC) traces for the fractionated and crude samples. Fractionation of the G3 copolymers was aided by centrifugation in order to maximize the recovery yield.

Linear Polyisoprenes. Linear polyisoprene samples with M_w ranging from 30 000 to 10^6 were prepared as reference materials for the rheological measurements. The linear polyisoprenes were synthesized under the same conditions used for the copolymers to achieve a similar chain microstructure. Molecular weight and microstructure characterization data for the linear polymers are provided as Supporting Information (Table S1).

Characterization. The apparent (polystyrene-equivalent) and absolute molecular weights of the polystyrene substrates and the arborescent copolymers were determined by size exclusion chromatography (SEC) analysis. The details of these procedures are provided as Supporting Information.

The composition of the copolymers was determined from ^{1}H NMR spectra obtained in $CDCl_3$ on a Bruker AC-300 nuclear magnetic resonance (NMR) spectrometer. ^{1}H NMR spectra of the polyisoprene side chain samples also allowed microstructure analysis by established methods.[11]

The glass transition temperature (T_g) of the polyisoprene side chains and the arborescent copolymers were measured with a TA Instruments differential scanning calorimeter (DSC) model Q100 equipped with a refrigerated cooling system, using the TA Instruments Universal Analysis 2000 software package. The samples (~10 mg) were dried under vacuum for 2 days and sealed in aluminum pans for the measurements. Each sample was equilibrated at −90 °C and scanned at a rate of 10 °C/min up to 120 °C. Duplicate scans were collected in the same temperature range to ensure reproducibility of the results. The T_g values reported correspond to the midpoint change in heat capacity in the transition region and were reproducible to within ±0.2 °C for successive scans.

Rheology. The polyisoprene samples used in the rheological measurements were stabilized with 0.25% w/w *N*,*N*′-diphenyl-1,4-phenylenediamine by dissolution in a 90/10 v/v mixture of pentane/THF. The stabilized samples were recovered by evaporation under vacuum of the solution over several days to constant mass.

Dynamic moduli were measured with a strain-controlled Rheometrics dynamic spectrometer RDS II, using the parallel plate geometry. The plate radius was 12.5 mm, and the plate gap was varied between 1.5 and 2.0 mm. Dynamic strain sweeps were performed at each temperature in order to determine the regime of linear viscoelasticity. Dynamic frequency sweeps from 100 to 0.01 rad/s were carried out at 20 °C intervals from −40 to 80 °C, using strains of 1−20%. The plate gap was adjusted at each temperature to compensate for thermally induced changes in sample thickness. The measurements were limited to 80 °C since chain cleavage is known to occur at higher temperatures in arborescent polymers based on acetyl coupling sites.[12] Repeat measurements were performed for each polymer on new samples using different plate gaps to ensure linearity. The master modulus−frequency curves were constructed by superposition of the storage (G') and loss moduli (G'') according to[13]

$$G'(\omega,T) = b_T G'(a_T\omega,T_0) \quad (1)$$

$$G''(\omega,T) = b_T G''(a_T\omega,T_0) \quad (2)$$

where ω is the radial frequency, a_T and b_T are the temperature-dependent frequency and modulus shift factors, and T_0 is the reference temperature (20 °C). Time−temperature superposition of the data was performed using the Rheometric Scientific RSI Orchestrator Software version V6.5.8, and master curves were obtained by a horizontal shifting method using vertical temperature and density compensation. The density of the samples at each temperature (ρ) was calculated from the density of natural rubber, according to

$$\rho = \frac{\rho_0}{1 + \Delta T\beta} \quad (3)$$

where ρ_0 is the density of natural rubber at 25 °C (913 kg/m^3), ΔT is the difference in temperature from 25 °C, and $\beta = 6.7 \times 10^{-4}$ K^{-1}.

Steady-stress creep experiments were performed to estimate the zero-shear viscosity (η_0) of the G2 copolymers, which could not be measured using the strain-controlled instrument. Using a stress-controlled Paar Physica DSR 4000 rheometer equipped with 12.5 mm radius parallel plates, the stress (σ) was varied between 400 and 2800 Pa (G1PS-cPIP5) or 100 and 2000 Pa (G1PS-cPIP30) at

Table 1. Characterization Data for Arborescent Polystyrene Substrates

sample	M_w^{br} [a]	M_w/M_n^{br} [a]	M_w [b]	f_w	CH_3CO-/mol %[c]	grafting sites
PS (linear)	6500	1.08			29	18
G0PS	4600	1.08	85 400	17	26	213
G1PS	5100	1.09	1050 000	190	27	2700
G2PS	5400	1.09	11 800 000	1900	22	25000

[a] Absolute values for the side chains determined by SEC analysis with DRI detection. [b] Absolute M_w of the graft polystyrenes determined by light scattering. [c] Acetylation level determined by ^{1}H NMR analysis.

Table 2. Characterization Data for Arborescent Isoprene Copolymers

	cPIP side chains		arborescent copolymers					
sample	M_w^{br} [a]	M_w/M_n^{br} [a]	M_w^{app} [b]	M_w[a]	M_w/M_n[a]	f_w	G_y/%[c]	C_e/%[d]
PS-cPIP5	4 860	1.08	73 000	94 200	1.03	18	83	100
PS-cPIP10	9 370	1.06	98 000	157 000	1.02	16	80	89
PS-cPIP30	33 900	1.06	350 000	446 000	1.01	14	64	72
PS-cPIP40	40 400	1.05	410 000	477 000	1.04	12	66	64
G0PS-cPIP5	4 950	1.09	290 000	1120 000	1.04	209	78	98
G0PS-cPIP10	9 830	1.07	370 000	2040 000	1.06	199	71	93
G0PS-cPIP30	28 100	1.06	1050 000[e]	4990 000	1.27[e]	170	61	82
G0PS-cPIP40	40 100	1.05	1060 000[e]	5450 000	1.37[e]	130	35	63
G1PS-cPIP5	4 800	1.07	1330 000[e]	13 000 000	1.40[e]	2500	64	91
G1PS-cPIP30	29 800	1.06		22 600 000		720	28	27
G2PS-cPIP5	4 810	1.07		42 700 000		6400	39	26
G2PS-cPIP30	27 500	1.06		53 100 000		1500	6	6

[a] Absolute values for the side chains and graft copolymers from SEC analysis with LS detection or batchwise LS measurements. [b] Apparent values determined using SEC calibrated with linear polystyrene standards. [c] Approximate grafting yield based on relative peak areas. [d] Coupling efficiency. [e] SEC apparent values determined with ultrahigh molecular weight columns corrected for band broadening.

20 °C. For each stress value the equilibrium strain rate ($\dot{\gamma}$) was measured and used to calculate the viscosity ($\sigma/\dot{\gamma}$). The zero-shear viscosity of each copolymer was estimated by extrapolation of the calculated viscosities to zero strain rate.[7c]

Results and Discussion

Synthesis. The characteristics of the polystyrene substrates used in the preparation of the graft copolymers are summarized in Table 1. The branching functionality of the polymers (f_w), defined as the number of chains added in the last grafting reaction, was calculated from the equation

$$f_w = \frac{M_w(G) - M_w(G-1)}{M_w^{br}} \quad (4)$$

where $M_w(G)$, $M_w(G-1)$, and M_w^{br} are the absolute weight-average molecular weight of the graft polymer of generation G, of the preceding generation, and of the side chains, respectively. For each grafting reaction the acetylation level (22−29 mol %) and the molecular weight of the side chains ($M_w^{br} \approx 5000$) were relatively constant. Coupling of the chains added in each grafting cycle can be expected to occur mainly on the side chains added in the previous grafting reaction due to the large increase in molecular weight in each cycle and the steric hindrance imposed by the large number of grafts present. The number of coupling sites on the substrates was calculated from their absolute molecular weight and acetylation level. Both f_w and the number of coupling sites increase nearly geometrically for successive generations.

Isoprene copolymers with a high proportion of *cis*-1,4-units were synthesized for the purpose of studying the rheological behavior of elastomeric arborescent polymers. A previous publication on the synthesis of arborescent isoprene copolymers from acetylated polystyrene substrates was limited to polyisoprene side chains with a mixed microstructure.[10] The polymerization and grafting reactions were performed in pure THF, which is optimal for the grafting reaction. In the present work, a high *cis*-1,4-isoprene units content was obtained by polymerization in cyclohexane (nonpolar solvent). Prior to grafting, a large volume of THF was added to the reactor to increase the polarity of the solvent mixture and the yield of the coupling reaction. The coupling yield of anionic grafting processes is negatively influenced by a decrease in polarity of the reaction medium.[14] This approach was also determined to be necessary for efficient coupling of *cis*-polyisoprene chains with chloromethylated polystyrene substrates.[8b] The grafting yield, defined as the fraction of the polyisoprene chains generated becoming coupled with the substrate, was found to decrease significantly in that study for higher generation substrates and for longer side chains. The inaccessibility of the coupling sites on the more rigid, highly branched substrates to the macroanions and the presence of residual protic impurities were suggested to justify the decreased grafting efficiency. Another factor potentially significant is the inherent immiscibility of the polystyrene and polyisoprene phases, further hindering the diffusion of the macroanions to the coupling sites. Similar results were obtained in the present work, the grafting yield decreasing to 39 and 6% for the G2PS-cPIP5 and G2PS-cPIP30, respectively (Table 2).

The characteristics of the arborescent isoprene copolymers synthesized are summarized in Table 2. The nomenclature used for the grafting substrates and the graft copolymers specifies their composition and structure. For example, G1PS-cPIP5 refers to a graft copolymer with *cis*-1,4-polyisoprene side chains of $M_w^{br} \approx 5000$ grafted onto a G1 (twice-grafted) arborescent polystyrene substrate. The compact structure of the arborescent copolymers is obvious from the underestimation of the apparent molecular weight (M_w^{app}) using SEC with a linear polystyrene standards calibration curve, as compared to the absolute weight-average molecular weight (M_w) determined with light scattering. Evidence for a narrow molecular weight distribution is seen in the low polydispersity index values obtained ($M_w/M_n = 1.01-1.06$). Copolymers with $M_w \geq 5 \times 10^6$ were analyzed using SEC columns with a pore size suitable for linear polystyrene samples to $M_w = 4 \times 10^7$. Significant peak broadening was observed with these columns even after the application of band broadening correction for G0PS-cPIP30, G0PS-cPIP40, and

Table 3. Polyisoprene Content and Microstructure Analysis for Linear Polyisoprenes and Arborescent Isoprene Copolymers

	PIP/% w/w			PIP microstructure/mol %		
sample	^{1}H NMR	M_w[a]	φ_{PS}[b] (%)	*cis*-1,4-	*trans*-1,4-	3,4-
PS-cPIP5	94	93	6.3	69	24	7
PS-cPIP10	95	96	3.6	69	21	10
PS-cPIP30	>98	99	0.89	71	23	7
PS-cPIP40	>98	99	0.89	73	20	7
G0PS-cPIP5	93	92	7.2	69	24	7
G0PS-cPIP10	95	96	3.6	70	20	10
G0PS-cPIP30	>98	98	1.8	71	22	7
G0PS-cPIP40	>98	98	1.8	73	20	7
G1PS-cPIP5	94	92	7.2	68	23	9
G1PS-cPIP30	>98	95	4.5	72	22	6
G2PS-cPIP5	90	72	26	68	23	9
G2PS-cPIP30	90	78	20	71	23	6

[a] Calculated from the difference in absolute M_w of the graft copolymer and polystyrene substrate. [b] Volume fraction of polystyrene in the molecules based on the molecular weight increase, and bulk densities $\rho_{PS} = 1030$ kg/m^3 and $\rho_{PIP} = 913$ kg/m^3 at 25 °C.

G1PS-cPIP5, as indicated by the larger apparent M_w/M_n values obtained. Despite band broadening, the SEC peaks obtained for these copolymers are consistent with a controlled architecture, as they are symmetrical and unimodal, and therefore free of side reactions such as cross-linking. The highest molecular weight samples ($M_w \geq 2 \times 10^7$) did not elute even from the high molecular weight SEC columns.

The method used to determine the branching functionality (f_w) of the copolymers in Table 2 is identical to that for the polystyrene substrates (eq 4) and represents the number of polyisoprene side chains in the molecules. The coupling efficiency (C_e), defined as the fraction of acetyl groups consumed in the grafting reaction, was calculated as the ratio of f_w to the number of potential coupling sites on the substrate (Table 1). Near quantitative reaction of the coupling sites was achieved for the G0 and G1 copolymers with short PIP arms ($M_w^{br} \approx 5000$, 10 000, $C_e > 90\%$). In contrast, the G0 and G1 copolymers with longer arms have lower than expected branching functionalities since the coupling efficiency decreased for increasing PIP arm molecular weight. The coupling reaction presumably proceeds only to the point where steric hindrance imposed by the attached PIP arms inhibits further grafting.[8c] Significantly lower coupling efficiencies were also attained for higher generation copolymers, again due to more pronounced steric effects. This is most obvious for sample G2PS-cPIP30, with $f_w = 1500$ as compared to the 25 000 coupling sites available on the substrate, representing a coupling efficiency of only 6%. Despite the low coupling yield, the molecular weight of the copolymer increased 4.5-fold upon grafting the PIP chains.

Composition analysis of the graft copolymers by ^{1}H NMR spectroscopy yielded polyisoprene contents varying from 90 to over 98 wt % (Table 3). Peaks corresponding to the polystyrene component are not detected for the majority of copolymers with long side chains ($M_w^{br} \approx 30\,000$, 40 000), represented by a polyisoprene content >98%. The polyisoprene contents were also estimated from the difference in absolute molecular weights of the graft copolymers and the corresponding polystyrene substrates and agree well with the ^{1}H NMR results for G0, G1, and G2 copolymers. The polyisoprene contents were clearly overestimated by ^{1}H NMR analysis for the G3 copolymers, presumably due to the differences in relaxation characteristics of the polyisoprene and the highly branched polystyrene components affecting the intensity of the peaks in the NMR spectra. While the polyisoprene content is high for all the copolymers, the polystyrene content varies widely among the samples, ranging from 1 to 28 wt % based on the absolute molecular weight difference. The corresponding volume fraction of the polystyrene core in the molecules ranges from 1 to 26 vol %, increasing for higher generations and for copolymers with shorter PIP side chains (Table 3).

Table 4. Glass Transition Temperature (T_g) Data for Linear Polyisoprenes, Polyisoprene Side Chain Samples, and Arborescent Isoprene Copolymers

sample	linear PIP/side chain T_g/°C[a]	arborescent copolymer T_g/°C[a]
cPIP30	−64.2	
cPIP110	−64.9	
cPIP130	−65.0	
cPIP340	−64.7	
cPIP1M	−64.6	
PS-cPIP5	−65.7	−64.2
PS-cPIP10	−63.7	−61.6
PS-cPIP30	−64.1	−62.4
PS-cPIP40	−63.5	−62.5
G0PS-cPIP5	−65.5	−63.6
G0PS-cPIP10	−64.3	−62.3
G0PS-cPIP30	−64.9	−64.0
G0PS-cPIP40	−64.3	−63.1
G1PS-cPIP5	−66.3	−63.2
G1PS-cPIP30	−65.2	−63.5
G2PS-cPIP5	−66.2	−63.1
G2PS-cPIP30	−64.6	−63.3

[a] Variation of ±0.2 °C for a minimum of two measurements.

The microstructure of the polyisoprene side chains derived from ^{1}H NMR analysis (Table 3) varied slightly from 68 to 73 mol % for the *cis*-1,4-units, from 20 to 24 mol % for the *trans*-1,4-units, and from 6 to 10 mol % for the 3,4-units. The microstructure variations observed are very minor and due to the different initiator and monomer concentrations used for each polymerization reaction. For the anionic polymerization of isoprene, an increase in initiator concentration or a decrease in monomer concentration both lead to a decrease in *cis*-1,4-units content relative to *trans*-1,4-units, without affecting the 3,4-units content significantly.[15] Indeed, a decrease in *cis*-1,4-content is observed for copolymers with shorter side chains (prepared at higher initiator concentrations). A more significant influence of initiator concentration is observed for the microstructure of the linear polyisoprenes (Table S1 in the Supporting Information). The proportion of *cis*-1,4-units varied from 71 mol % (cPIP30) to 78 mol % (cPIP1M) in this case due to the decreased initiator and increased monomer concentrations required to prepare the high molecular weight linear polymers.

Thermal Properties. The glass transition temperatures (T_g) measured by DSC analysis for linear polyisoprenes (reference materials), the polyisoprene side chain samples, and the isoprene copolymer samples are compared in Table 4. The T_g values measured for the linear polyisoprenes are virtually independent of molecular weight (−64.2 to −65.0 °C) and do not appear to be sensitive to small changes in microstructure within the range investigated. Even for the polyisoprene side-chain samples T_g variations are minor (2.6 °C), in spite of their lower molecular weight. This is not unexpected since the side-chain molecular weights are all above the critical molecular weight for T_g insensitivity in polyisoprenes ($M_c \approx 2500$).[16] The T_g values measured for the polyisoprene component of the copolymers were only 1−2 °C higher than for the corresponding side-chain samples. This slight increase may be a result of reduced chain mobility upon anchoring of the polyisoprene side chains to the substrate or else to limited miscibility between the core and shell components. The polyisoprene chains appear to be mainly phase-separated from the polystyrene cores since a much larger

shift in T_g would be expected for significant phase mixing, in particular for copolymers with a significant polystyrene content. Microphase separation has been reported previously based on DSC and ^{13}C NMR studies of polystyrene-*cis*-1,4-polyisoprene diblock copolymers.[17] Thus, a phase-separated core−shell morphology can be envisioned for the arborescent polystyrene-*graft*-polyisoprene copolymers, in agreement with previous results of an AFM imaging investigation.[8b] No T_g corresponding to the polystyrene cores was detected for any of the isoprene copolymers, even for the highest generation copolymers with polystyrene contents of up to 28% w/w. To ensure that this was the case, the DSC analysis was also performed on larger samples, and a broad temperature range around 100 °C was carefully monitored. A previous study of arborescent polystyrenes by DSC showed that the transition regions broadened and decreased in magnitude for higher generation polymers[6a] due to decreased chain mobility within the highly branched molecules. This may explain the lack of a transition for the polystyrene cores in the copolymers.

Rheology. Two distinct regions are generally observed in modulus−frequency curves for linear high molecular weight polymers in the molten state.[13] A relatively flat plateau region is present at high and intermediate frequencies due to large-scale motions of the molecules being restricted by entanglements. The breadth of the plateau region increases with molecular weight. The low-frequency or terminal region is associated with viscous flow of the polymer, involving motions of the entire molecules. Reptation motions of a chain along its entangled length most effectively describe the terminal relaxation process.[18] The rheological behavior of branched polymers differs significantly from that of linear polymers. Intuitively, relaxation of the branched molecules by a simple reptation mechanism is impossible. Path breathing[19] and constraint release[2b,20] mechanisms have been proposed as alternate, more acceptable models for the relaxation of star and comb-branched molecules. More highly branched polymers, such as dendrimers and hyperbranched polymers, behave as polymer fractals due to a lack of entanglements between the compact molecules.[9] The main focus of the current study was the rheological characterization of arborescent isoprene copolymers for comparison with other branched polymers.

Dynamic mechanical measurements were performed on the arborescent isoprene copolymers in order to study the influence of generation number, branch length, and composition on the viscoelastic properties of highly branched elastomers. Rheological testing was performed at temperatures up to 80 °C, as thermally induced cleavage of the chains is known to occur at elevated temperatures for arborescent polymers prepared from acetylated grafting substrates.[12] Despite this limitation, the range of temperatures used for the frequency sweeps produced modulus−frequency master curves spanning up to 8 decades of frequencies, and terminal flow was observed for all G0 and G1 copolymers.

Arborescent isoprene copolymers of overall generation G0 (comb structures) contain 12−18 polyisoprene arms (Table 2) coupled with a short linear polystyrene chain ($M_w \approx 5000$). This architecture resembles that of star polymers, in particular for long polyisoprene side chains, since the relatively short polystyrene chain acts as a central branching point. Star polymer-like rheological behavior is expected, particularly below the T_g of the polystyrene core, since only motions of the polyisoprene side chains can be detected in the rheological measurements. The modulus−frequency curves of the G0 copolymers (Figure 2) strongly resemble those obtained for linear polyisoprenes and

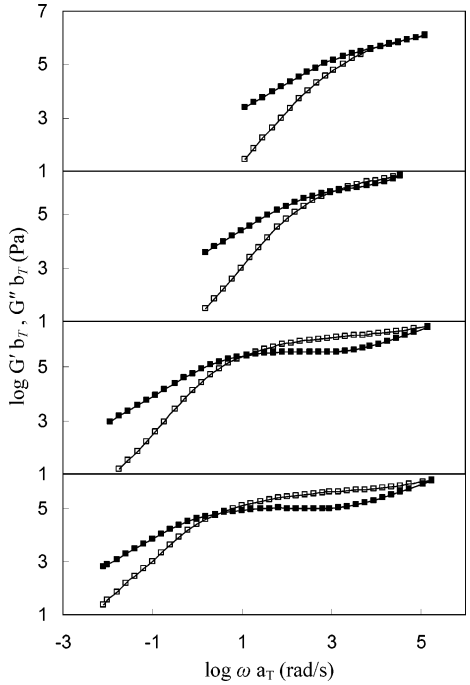

Figure 2. Dynamic modulus curves G' (□) and G'' (■) at 20 °C. From top to bottom: PS-cPIP5, PS-cPIP10, PS-cPIP30, and PS-cPIP40.

also bear a resemblance to those reported for star-branched polymers[1b,21] and G0 (comb-branched) arborescent polystyrenes.[7c] The entanglement plateau is absent for PS-cPIP5 since the molecular weight of the side chains is somewhat lower than the critical entanglement molecular weight for polyisoprene ($M_e = 5400$).[22] The modulus curves for copolymers with longer polyisoprene arms (PS-cPIP10, PS-cPIP30, PS-cPIP40) display a plateau indicating entanglement coupling, which becomes more pronounced for increasing arm length. In the terminal region the comb-branched copolymers display normal limiting behavior, with G' and G'' having slopes of +2 and +1 on the log−log plots, respectively. The terminal relaxation is shifted to lower frequencies as the molecular weight of the polyisoprene arms increases.

The first-generation arborescent isoprene copolymers (G1 structure overall) comprise 130−210 polyisoprene arms (Table 2) coupled to a comb-branched (once grafted) G0 polystyrene core. The modulus−frequency curves of the G1 copolymers (Figure 3) bear a striking resemblance to those reported previously for G1 arborescent polystyrenes[7c] and for star-branched polybutadienes with up to 270 branches.[20] The two inflection points observed in the G'' curve for all G1 copolymers, one at intermediate frequencies and one at low frequencies, are attributed to relaxation of the polyisoprene arms and of the entire molecules, respectively. These inflections are shifted to longer times (lower frequencies) for increasing polyisoprene arm molecular weights. Each spectrum displays normal terminal behavior (slope of $G' = +2$, $G'' = +1$), the terminal relaxation being shifted to lower frequencies with increasing PIP arm molecular weight.

The modulus−frequency curves for arborescent isoprene copolymers of the second (G2) and third generations (G3) display behaviors markedly different from the G0 and G1 copolymers (Figure 4). This change in rheological behavior was also noticed for G2 and G3 arborescent polystyrenes as compared to the G0 and G1 analogues.[7c] The storage modulus (G') for the G2 copolymers is larger than the loss modulus (G'') over the entire frequency range. At low frequencies G' reaches

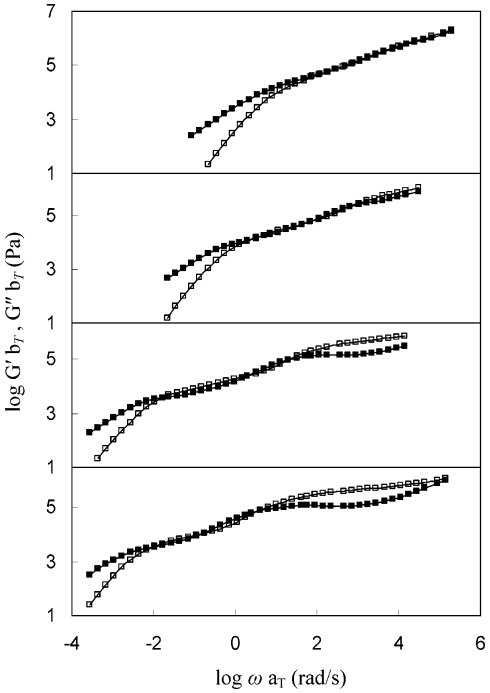

Figure 3. Dynamic modulus curves G' (□) and G'' (■) at 20 °C. From top to bottom: G0PS-cPIP5, G0PS-cPIP10, G0PS-cPIP30, and G0PS-cPIP40.

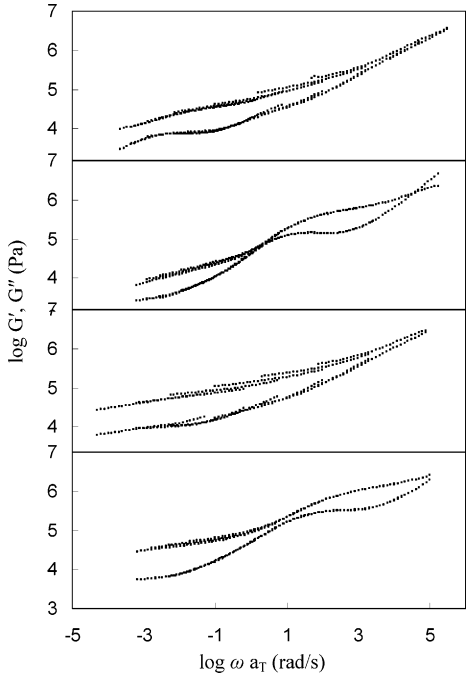

Figure 4. Dynamic modulus curves G' (upper) and G'' (lower) at 20 °C. From top to bottom: G1PS-cPIP5, G1PS-cPIP30, G2PS-cPIP5, and G2PS-cPIP30.

a plateau, while G'' is significantly smaller. These features are most pronounced in the master curve for the highest generation (G3) copolymers. Similar rheological features were observed for cross-linked polymer networks at the gel point[23,24] and for linear polyisoprenes with fillers.[25,26] An inflection point is also present in the G'' curves for G1PS-cPIP30 and G2PS-cPIP30 in Figure 4 at approximately the same frequency. These inflections appear at frequencies similar to the G0 and G1 copolymers with $M_w \approx 30\,000$ arms and are attributed to the relaxation of the polyisoprene arms.

Partial failure of the time−temperature superposition (TTS) principle is observable in the modulus curves for G1PS-cPIP5 and G2PS-cPIP5 in Figure 4. Vertical and horizontal shifting of the data to single curves using identical shift factors for G' and G'' was not possible for the G2 and G3 copolymers with short polyisoprene arms, particularly at intermediate and low frequencies. Interestingly, the modulus data at high frequencies (low temperatures) obeyed TTS. The modulus data collected at all temperatures were included in Figure 4 to illustrate this abnormal behavior. Blends of immiscible polymers are known not to obey TTS due to the different temperature dependencies of both components.[27] Departures from TTS have also been reported for both filled[28] and nonfilled[29] styrene−butadiene rubber (SBR), a two-phase system in which the polystyrene component is present as separate aggregated domains embedded in a continuous polybutadiene matrix. For nonfilled SBR, superposition of the modulus data measured above a critical temperature ($T \approx 15$ °C) required shift factors that differed significantly from normal relations.[29] It was argued that the polystyrene domains acted like inert filler particles below the characteristic temperature but contributed to the modulus significantly above this temperature, resulting in thermorheological complexity. Since temperature-dependent TTS failure was also observed in the present work, it appears that the polystyrene cores behave in a fashion similar to the phase-separated polystyrene domains present in SBR. The G1 and G2 polystyrene cores act as phase-separated domains on the basis of the DSC results presented earlier and previous AFM measurements.[8b,10] The volume fraction of the polystyrene cores in the G1PS ($\varphi_{PS} = 7.2\%$) and G2PS ($\varphi_{PS} = 26\%$) copolymers with short polyisoprene arms ($M_w \approx 5000$) appears to be sufficiently large to contribute to the overall modulus. However, the modulus curves for copolymers containing long arms ($M_w \approx 30\,000$) based on the same cores ($\varphi_{PS} = 4.5\%$ for G1PS-cPIP30, $\varphi_{PS} = 20\%$ for G2PS-PIP30) and those for the lower generation copolymers all obey the TTS. The volume fraction of the polystyrene core and the length of the polyisoprene arms therefore *both* appear to be important factors affecting TTS fitting of the rheological data.

The horizontal frequency shift factors (a_T) used to fit the modulus curve segments for the linear polyisoprenes and the isoprene copolymers in a temperature range of −40 to 80 °C were described by the WLF equation

$$\log a_T = \frac{-c_1(T - T_0)}{c_2 + (T - T_0)} \tag{5}$$

with $T_0 = 20$ °C. The WLF parameters $c_1 = 4.93 \pm 0.15$ and $c_2 = 132 \pm 4$ K were determined as the average of all shift parameters for the five linear polyisoprene samples (Figure S1, provided as Supporting Information). These parameters are consistent with literature values for linear polyisoprenes with a similar microstructure ($c_1 = 4.1$, $c_2 = 122$ K, $T_0 = 25$ °C)[30] when compared at the same reference temperature.[13] The WLF parameters used to fit the modulus data for isoprene copolymers with long arms ($M_w \approx 30\,000$ or $40\,000$) are compared to the average values measured for the linear polyisoprenes in Figure 5. Excellent agreement was found between WLF parameters used to fit the linear polymers and the copolymers with long polyisoprene arms. The standard deviations are not included in the plot, as they are smaller than the size of the symbols.

The WLF parameters for copolymers with the shorter polyisoprene arms ($M_w \approx 5000$ or $10\,000$) are more variable

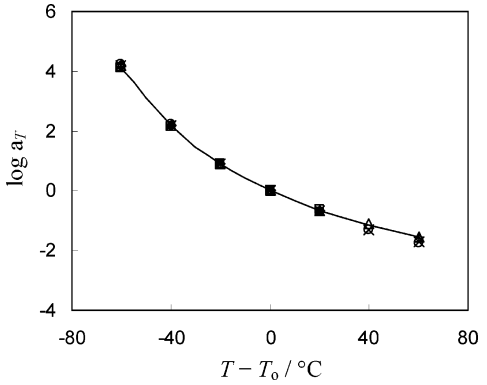

Figure 5. Frequency shift factors (a_T) for isoprene copolymers with $M_w \approx 30\,000$ or 40 000 polyisoprene arms ($T_0 = 20$ °C): (□) PS-cPIP30, (◇) PS-cPIP40, (△) G0PS-cPIP30, (+) G0PS-cPIP40, (×) G1PS-cPIP30, (○) G2PS-cPIP30, and (−) average values for linear polyisoprenes.

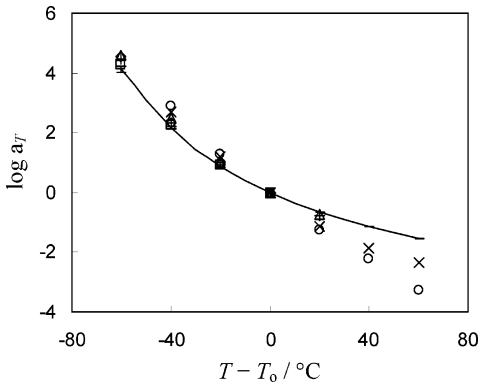

Figure 6. Frequency shift factors (a_T) for isoprene copolymers with $M_w \approx 5000$ or 10 000 polyisoprene arms ($T_0 = 20$ °C): (□) PS-cPIP5, (△) G0PS-cPIP5, (×) G1PS-cPIP5, (○) G2PS-cPIP5, (◇) PS-cPIP10, (+) G0PS-cPIP10, and (−) average for linear polyisoprenes with standard deviations.

than for the other polymers, as illustrated in Figure 6. Although the TTS can be used to effectively superimpose the modulus curves for most copolymers, the different WLF parameters obtained for the short-side-chain materials suggest that they behave more like heterogeneous copolymers of polystyrene and polyisoprene. The copolymers with long arms behave essentially like highly branched isoprene homopolymers.

It was pointed out earlier that the dynamic modulus−frequency curves for arborescent copolymers contain inflection points revealing the existence of different relaxation mechanisms for these highly branched molecules. Similar observations were reported for star,[1a] comb,[2a] and star−comb polymers.[2b] The inflections at intermediate frequencies are generally associated with motions of the branches, while those at low frequencies are related to whole molecule motions. The side-chain equilibration time $\tau_{G''_{max}} = 1/\omega_{G''_{max}}$, corresponding to the time required for branch relaxation, can be estimated from the maximum in G'' at intermediate frequencies.[20] The $\tau_{G''_{max}}$ values determined for the G0−G3 copolymers are listed in Table 5. For copolymers containing polyisoprene arms of comparable molecular weight (M_w^{br}), the side-chain equilibration time is nearly constant for different generations. The maxima at intermediate frequencies are therefore unambiguously related to motions of the polyisoprene side chains. Only one relaxation was observed in the modulus curves for the G0 copolymers with short side chains ($M_w \approx 5000$ or 10 000), and consequently $\tau_{G''_{max}}$ values could not be estimated.

The relaxation times associated with the modulus−frequency curves of the G0 and G1 copolymers were calculated by fitting a generalized Maxwell model to the experimental curves of the dynamic viscosities $\eta'(\omega)$ and $\eta''(\omega)$,[31] as previously done for arborescent styrene homopolymers,[7c] using the equations

$$\eta'(\omega) = \eta'_\infty + G_m \sum_{i=1}^{M} \frac{\tau_{m,i}}{1 + \omega^2 \tau_{m,i}^2} + G_n \sum_{j=1}^{N} \frac{\tau_{n,j}}{1 + \omega^2 \tau_{n,j}^2} \quad (6)$$

$$\eta''(\omega) = G_m \sum_{i=1}^{M} \frac{\omega \tau_{m,i}^2}{1 + \omega^2 \tau_{m,i}^2} + G_n \sum_{j=1}^{N} \frac{\omega \tau_{n,j}^2}{1 + \omega^2 \tau_{n,j}^2} \quad (7)$$

where η'_∞ represents the storage viscosity at very high frequencies and ω is the frequency. Two groups of long ($\tau_{m,i}$) and short ($\tau_{n,j}$) relaxation times were entered in eqs 6 and 7 with their respective relaxation strengths (G_m and G_n). Each group of relaxation times in eqs 6 and 7 is expressed relative to the longest time for each relaxation mode $\tau_{m,1}$ and $\tau_{n,1}$ as two series of 6−10 values, generated from $\tau_{m,i} = \tau_{m,1}/i^2$ and $\tau_{n,j} = \tau_{n,1}/j^2$. The equations can be used to model dynamic viscosity curves where two distinct relaxation modes are observed. The experimental dynamic viscosity curves for the linear polyisoprenes and the G0 copolymers with short polyisoprene arms (PS-cPIP5, PS-cPIP10) were fitted with a single group of relaxation times, as summarized in Table 5. Two groups of relaxation times were required to fit the data for the G0 copolymers with long side chains (PS-cPIP30, PS-cPIP40) and all the G1 copolymers. The fitting errors provided in Table 5, calculated as the standard deviation between the calculated and experimental viscosities, were below 10% for all G0 and G1 copolymers. Fitting of the linear polymers was poor, in particular for higher molecular weight samples, which display a broad entanglement plateau. The measured and calculated η' and η'' curves for G0PS-cPIP10 are provided in Figure 7 as an example. The curves for the G2 and G3 copolymers could not be modeled using two distinct groups of relaxation times, suggesting that multiple relaxations occur in these highly branched molecules at intermediate and low frequencies.

The limiting properties of model branched polymers such as stars and combs depend on the molecular weight of the arms and in particular on the number of entanglements per arm.[2a,20] The terminal relaxation times $\tau_{m,1}$ of the G0 and G1 copolymers (Table 5) displayed a similar dependence on arm molecular weight (M_w^{br}). The short time relaxation $\tau_{n,1}$, observed at intermediate frequencies for G0 copolymers with long side chains and all G1 copolymers, is associated with movements of the polyisoprene side chains. For the limited number of results available, comparable short time relaxations $\tau_{n,1}$ are indeed present for G0 and G1 copolymers with polyisoprene arms of equivalent molecular weight ($M_w \approx 30\,000$ or 40 000), in qualitative agreement with the $\tau_{G''_{max}}$ results. However, the $\tau_{n,1}$ values are systematically larger since they represent the longest relaxation time in the group used to fit the experimental data. The $\tau_{G''_{max}}$ values are smaller because they represent the peak value for each relaxation event. Relaxations related to motions of the branches in the G0 copolymers with short side chains were not observed, but the existence of a closely located relaxation not resolved from the terminal relaxation cannot be excluded.

The zero-shear viscosity η_0 of the G0 and G1 copolymers and linear polyisoprene samples was determined from the

Table 5. Rheological Data for Linear Polyisoprenes and Arborescent Isoprene Copolymers

sample	$\tau_{G''_{max}}$[a]/ s	$\tau_{n,1}$[b]/s	N[c]	$\tau_{m,1}$[d]/s	M[c]	fitting error[e]/% η'	fitting error[e]/% η''
cPIP30	1.3×10^{-3}			2.5×10^{-3}	4	21 (43)	17 (51)
cPIP110	4.0×10^{-2}			0.30	8	28 (70)	19 (47)
cPIP130	0.10			0.55	7	31 (73)	19 (51)
cPIP340	1.6			16	6	52 (93)	19 (45)
cPIP1M	50						
PS-cPIP5				7.9×10^{-4}	7	4.0 (16)	9.8 (40)
PS-cPIP10				5.0×10^{-3}	7	3.1 (19)	5.7 (22)
PS-cPIP30	7.9×10^{-3}	0.10	10	0.42	7	8.2 (43)	7.9 (27)
PS-cPIP40	1.6×10^{-2}	2.7	10	1.7	6	6.3 (35)	6.9 (34)
G0PS-cPIP5	1.3×10^{-4}	5.0×10^{-4}	10	0.17	10	2.2 (13)	6.0 (25)
G0PS-cPIP10	1.3×10^{-3}	3.2×10^{-3}	7	2.1	8	2.9 (11)	5.4 (36)
G0PS-cPIP30	1.0×10^{-2}	0.14	10	160	6	7.5 (38)	5.8 (34)
G0PS-cPIP40	2.0×10^{-2}	0.55	7	320	5	7.8 (45)	5.2 (25)
G1PS-cPIP5							
G1PS-cPIP30	6.3×10^{-3}						
G2PS-cPIP5							
G2PS-cPIP30	6.3×10^{-3}						

[a] Average relaxation times associated with the motions of the branches, estimated from a maximum in the G''curves. [b] Longest relaxation times associated with the motions of the branches. [c] Total number of Maxwell elements used to fit each group of relaxation times. [d] Longest terminal relaxation times associated with whole molecule motions. [e] Standard deviation for Maxwell model fit of dynamic viscosity data. The maximum deviation is shown in parentheses.

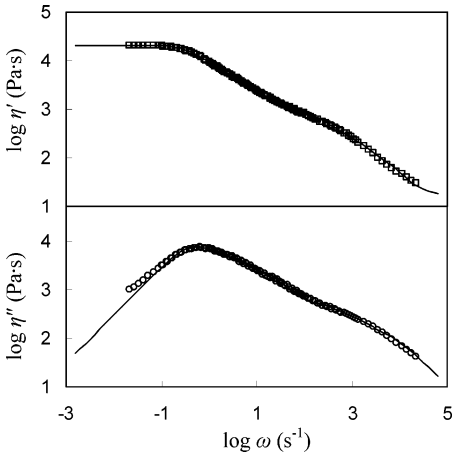

Figure 7. Dynamic viscosity curves of G0PS-cPIP10: η' (□), η'' (○), and (−) model fitting of the data.

terminal portion of the loss modulus, where the G'' curve reaches a limiting slope value of unity, according to the equation

$$\eta_0 = \lim_{\omega \to 0} \frac{G''(\omega)}{\omega} \tag{8}$$

As limiting values were not reached for the G2 copolymers, their zero-shear viscosity was determined from steady-stress creep measurements as explained in the Experimental Section. The steady-stress measurements could not be carried out with the G3 copolymers since sufficiently low strain rates could not be attained to allow extrapolation of the measured viscosity for these materials.

The zero-shear viscosity of the G0 and G1 copolymers displays a dependence on arm molecular weight (M_w^{br}) similar to that observed for the terminal relaxation times $\tau_{m,1}$. The η_0 values for the G0, G1, and G2 copolymers are compared with linear polyisoprenes as a function of molecular weight in Figure 8. The viscosity of the linear polyisoprene samples at 20 °C is described by the equation $\eta_0 = 1.84 \times 10^{-13} M^{3.58}$, in excellent agreement with published results for linear polyisoprenes of comparable microstructure at 25 °C ($\eta_0 = 2.37 \times 10^{-13} M^{3.59}$).[30] The G0 and G1 copolymers have a lower η_0 than linear polyisoprenes of similar molecular weight, as expected for these very compact molecules. The scaling of η_0 could be approximated by straight lines having slopes of 3.5 and 4.0 for the G0 and G1 copolymers, respectively. Similar scaling relations were found for star-branched polystyrenes[1b] and polybutadienes[21] containing arms with a molecular weight comparable to the entanglement molecular weight (M_e) of the corresponding linear polymers. Interestingly, further enhancement in η_0 was observed for the star-branched systems once the number of entanglements per arm (M_{arm}/M_e) exceeded 3−5.[20] The rapid increase in viscosity observed was attributed to decreased reptation along the entangled arms. Even though the scaling of η_0 was approximated by a straight line for the G0 and G1 isoprene copolymers, there appears to be a slight upturn in Figure 8 for isoprene copolymers with longer arms (higher M_w), as would be expected for enhanced entanglement formation between the polyisoprene arms of adjacent molecules. Only the initial portion of an upturn is (arguably) apparent for the arborescent isoprene copolymers used in the present study, in spite of their side chain molecular weight being up to 8 times larger than $M_e = 5100$ for *cis*-1,4-polyisoprene.[22] In contrast, the star polymers investigated previously had M_w^{br} values up to 23 times larger than $M_e = 1800$ for 1,4-polybutadiene,[22] which led to an obvious upturn in plots of viscosity vs molecular weight due to their higher degree of entanglement. A similar viscosity enhancement phenomenon was observed for hyperbranched polyisobutylenes with branches having a ratio M_{arm}/M_e up to 10.[9c]

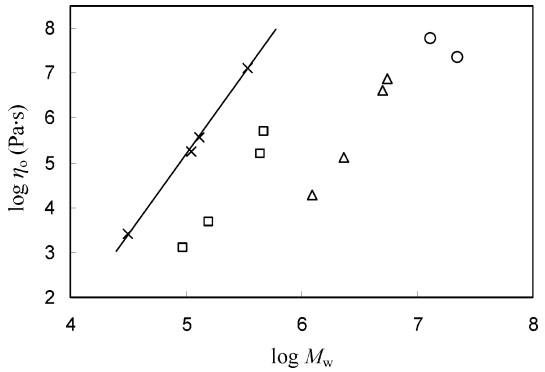

Figure 8. Zero-shear viscosity scaling: (×) linear polyisoprenes, (□) G0 copolymers, (△) G1 copolymers, and (○) G2 copolymers.

Irrespective of the possible presence of an upturn in the viscosity−molecular weight curve, the scaling behavior of the

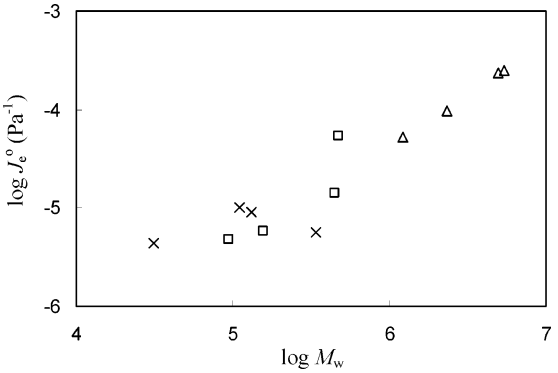

Figure 9. Zero-shear compliance at 20 °C: (×) linear polyisoprenes, (□) G0 copolymers, and (△) G1 copolymers.

isoprene copolymers is markedly different from the relation $\eta_0 \propto M_w^1$ determined for arborescent polystyrenes at 170 °C, which was attributed to a lack of entanglements between the molecules.[7c] This argument was reasonable because the molecular weight of the arms in the arborescent polystyrenes ($M^{br} \approx 5000$, 10 000, or 20 000) was below the critical entanglement molecular weight for linear polystyrene ($M_e \approx 13\,000$) in most cases.[22] A similar scaling behavior observed for polyether dendrimers,[9a] polyamidoamine dendrimers,[9b] and hyperbranched polyesters[9d] was likewise attributed to the lack of entanglements in these highly branched polymers. A dramatic change in behavior is observed for G2 arborescent isoprene copolymers, in analogy to the G2 arborescent polystyrenes, as η_0 decreased for increasing molecular weights. This change in behavior was attributed to the dominant influence of branching density within the molecules.[7c] The G2 molecules, containing the largest number of branching points, are characterized by higher η_0 values than the G0 and G1 polymers. Arm relaxation within these rigid molecules should be hampered, hindering reptation motions of chain segments and inhibiting configurational renewal of the molecule as a whole. The zero-shear viscosity of sample G1PS-cPIP5 (short arms) is nearly 3 times higher than for G1PS-cPIP30 (long arms), presumably due to the higher branching density of the copolymer with short arms. This reflects a change in behavior of the generation G2 copolymers from a relatively flexible branched structure to a more rigid, denser globular morphology.

The zero-shear recoverable compliance J_e^0 of the G0 and G1 copolymers and the linear polyisoprene samples was determined from the terminal portion of the storage modulus curves, where G' reached a limiting slope of 2, according to the equation

$$J_e^0 = \frac{1}{\eta_0^2} \lim_{\omega \to 0} \frac{G'(\omega)}{\omega^2} \tag{9}$$

corresponding to the extrapolation of a plot of $G'(\omega)/\omega^2$ to zero frequency. The low-frequency portion of the $G'(\omega)/\omega^2$ curve was fitted to a single-exponential decay to obtain an estimate of the compliance value.[32] The compliance of the linear polyisoprene samples ranged from 0.44×10^{-5} to 1.0×10^{-5} Pa^{-1} (Figure 9) and was essentially independent of molecular weight, as expected for linear polyisoprenes above the characteristic molecular weight $M_c' \approx 50\,000$. In spite of the significant scattering in the J_e^0 values determined by extrapolation, the compliance values obtained for the linear polyisoprenes are relatively constant across the limited molecular weight range investigated. A very different behavior is observed for the branched copolymers (Figure 9), as compliance increases nearly monotonically with molecular weight for both the G0 and G1 copolymer series. Sample G0PS-cPIP40 has a compliance value of 2.5×10^{-4} Pa^{-1}, more than 1 order of magnitude higher than linear polyisoprenes. Similar compliance values have been reported for star-branched polybutadienes ($(0.65-3.1) \times 10^{-4}$ Pa^{-1})[20] and for dendritically branched polystyrenes ($(0.10-1.2) \times 10^{-4}$ Pa^{-1})[32] within the same molecular weight range and are a clear indication of enhanced entanglement formation. The arborescent polystyrene-*graft*-polyisoprenes display a high degree of elasticity as compared to linear polyisoprenes. The combination of low viscosity and high elasticity of the arborescent copolymers may be interesting in terms of applications as rheological modifiers.

Conclusions

The dynamic mechanical behavior of arborescent polystyrene-*graft*-polyisoprenes was investigated as a function of side-chain length and generation number. The modulus−frequency curves obtained for the G0 and G1 copolymers displayed features similar to those found in other branched polymers such as star- and comb-branched systems. The modulus−frequency curves of the G2 and G3 copolymers displayed very different features similar to microgel or filled polymer systems. The significant change in behavior was attributed to a transition from a flexible branched structure (for generations G0 and G1) to a spherical rigid structure for generations G2 and above. This change in behavior at generation G2 is consistent with observations in both arborescent polystyrenes[6a,33] and arborescent polybutadienes[34] using intrinsic viscosity and light scattering measurements. Evidence for a heterogeneous morphology was seen in the thermorheological complexity of higher generation copolymers. Time−temperature superposition of the data onto one single master curve could not be achieved for G2 and G3 copolymers with short arms, as they apparently have a volume fraction of polystyrene sufficient to contribute to the overall modulus of the material. The arborescent isoprene copolymers have a low zero-shear viscosity as compared to linear polyisoprenes of identical molecular weights. The terminal relaxation times and zero-shear viscosities of the G0 and G1 copolymers increase with polyisoprene arm molecular weight, but the terminal properties of G2 copolymers are strongly influenced by the branching density. The increased terminal relaxation times of the G2 and G3 copolymers are attributed to hindered configurational renewal of the molecules due to increased structural stiffness. A slight upturn in the zero shear viscosity η_0 vs molecular weight curves for the G0 and G1 copolymers with longer arms suggests the onset of enhanced entanglement. The zero-shear compliance J_e^0 increased nearly monotonically with molecular weight for the G0 and G1 copolymers, in contrast to linear polyisoprenes for which J_e^0 was independent of molecular weight.

Acknowledgment. The authors thank Bruce Rudolph of Maple Instruments for the loan of rheology equipment and technical assistance, Jasmin Bhatia for help with synthesis, and the Natural Sciences and Engineering Research Council of Canada (NSERC), 3M Canada, and Imperial Oil Ltd. for financial support.

Supporting Information Available: Molecular weight characterization data for linear polyisoprenes, frequency shift factors (a_T) for linear polyisoprenes, and raw rheological data. This material is available free of charge via the Internet at http://pubs.acs.org.

References and Notes

(1) (a) Kraus, G.; Gruver, J. T. *J. Polym. Sci., Part A* **1965**, *3*, 105. (b) Graessley, W. W.; Roovers, J. *Macromolecules* **1979**, *12*, 959. (c)

Pearson, D. S.; Helfand, E. *Macromolecules* **1984**, *17*, 888. (d) Roovers, J. *Polymer* **1985**, *26*, 1091. (e) Adams, C. H.; Hutchings, L. R.; Klein, P. G.; McLeish, T. C. B.; Richards, R. W. *Macromolecules* **1996**, *29*, 5717. (f) Santangelo, P. G.; Roland, C. M; Puskas, J. E. *Macromolecules* **1999**, *32*, 1972.

(2) (a) Roovers, J.; Graessley, W. W. *Macromolecules* **1981**, *14*, 766. (b) Roovers, J.; Toporowski, P. *Macromolecules* **1987**, *20*, 2300. (c) Daniels, D. R.; McLeish, T. C. B.; Crosby, B. J.; Young, R. N.; Fernyhough, C. M. *Macromolecules* **2001**, *34*, 7025. (d) Kapnistos, M.; Vlassopoulos, D.; Roovers, J.; Leal, L. G. *Macromolecules* **2005**, *38*, 7852.

(3) Tomalia, D. A.; Hedstrand, D. M.; Ferritto, M. S. *Macromolecules* **1991**, *24*, 1435.

(4) Gauthier, M.; Möller, M. *Macromolecules* **1991**, *24*, 4548.

(5) Teertstra, S. J.; Gauthier, M. *Prog. Polym. Sci.* ***2004***, *29*, 277.

(6) (a) Gauthier, M.; Li, W.; Tichagwa, L. *Polymer* **1997**, *38*, 6363. (b) Choi, S.; Briber, R. M.; Bauer, B. J.; Topp, A.; Gauthier, M.; Tichagwa, L. *Macromolecules* **1999**, *32*, 7879. (c) Striolo, A.; Prausnitz, J. M.; Bertucco, A.; Kee, R. A.; Gauthier, M. *Polymer* **2001**, *42*, 2579.

(7) (a) Sheiko, S. S.; Gauthier, M.; Möller, M. *Macromolecules* **1997**, *30*, 2343. (b) Choi, S.; Briber, R. M.; Bauer, B. J.; Liu, D. W.; Gauthier, M. *Macromolecules* **2000**, *33*, 6495. (c) Hempenius, M. A.; Zoetelief, W. F.; Gauthier, M.; Möller, M. *Macromolecules* **1998**, *31*, 2299.

(8) (a) Gauthier, M.; Tichagwa, L.; Downey, J. S.; Gao, S. *Macromolecules* **1996**, *29*, 519. (b) Kee, R. A.; Gauthier, M. *Macromolecules* **1999**, *32*, 6478. (c) Kee, R. A.; Gauthier, M. *Macromolecules* **2002**, *35*, 6526.

(9) (a) Hawker, C. J.; Farrington, P. J.; Mackay, M. E.; Wooley, K. L.; Fréchet, J. M. J. *J. Am. Chem. Soc.* **1995**, *117*, 4409. (b) Uppuluri, S.; Morrison, F. A.; Dvornic, P. R. *Macromolecules* **2000**, *33*, 2551. (c) Robertson, C. G.; Roland, C. M.; Paulo, C.; Puskas, J. E. *J. Rheol.* **2001**, *45*, 759. (d) Suneel; Buzza, D. M. A.; Groves, D. J.; McLeish, T. C. B.; Parker, D.; Keeney, A. J.; Feast, W. J. *Macromolecules* **2002**, *35*, 9605.

(10) Li, J.; Gauthier, M.; Teertstra, S. J.; Xu, H.; Sheiko, S. S. *Macromolecules* **2004**, *37*, 795.

(11) (a) Essel, A.; Pham, Q. T. *J. Polym. Sci., Part A1: Polym. Chem.* **1972**, *10*, 2793. (b) Tanaka, Y.; Takeuchi, Y.; Kobayashi, M.; Tadokoro, H. *J. Polym. Sci., Part A2: Polym. Phys.* **1971**, *9*, 43.

(12) Gauthier, M.; Li, J.; Parent, S. R.; Teertstra, S. J. US 6,407,169 B1, 2002.

(13) Ferry, J. D. *Viscoelastic Properties of Polymers*, 3rd ed.; Wiley: New York, 1980; p 267.

(14) (a) Takaki, M.; Asami, R.; Ichikawa, M. *Macromolecules* **1977**, *10*, 850. (b) Takaki, M.; Asami, R.; Kuwata, Y. *Polym. J.* **1979**, *11*, 425.

(15) Worsfold, D. J.; Bywater, S. *Macromolecules* **1978**, *11*, 582.

(16) Cowie, J. M. G. *Eur. Polym. J.* **1975**, *11*, 297.

(17) Morèse-Séguéla, B.; St-Jacques, M.; Renaud, J. M.; Prud'homme, J. *Macromolecules* **1980**, *13*, 100.

(18) Graessley, W. W. *Adv. Polym. Sci.* **1982**, *47*, 67.

(19) Graessley, W. W. *Macromolecules* **1982**, *15*, 1164.

(20) Roovers, J. *J. Non-Cryst. Solids* **1991**, *131*−*133*, 793.

(21) Toporowski, P. M.; Roovers, J. *J. Polym. Sci., Part A: Polym. Chem. Ed.* **1986**, *24*, 3009.

(22) Fetters, L. J.; Lohse, D. J.; Richter, D.; Witten, T. A.; Zirkel, A. *Macromolecules* **1994**, *27*, 4639.

(23) Chambon, F.; Winter, H. H. *J. Rheol.* **1987**, *31*, 683.

(24) Winter, H. H. *Prog. Colloid Polym. Sci.* **1987**, *75*, 104.

(25) Gurovich, D.; Macosko, C. W.; Tirrel, M. *Rubber Chem. Technol.* **2004**, *76*, 1.

(26) Gurovich, D.; Macosko, C. W.; Tirrel, M. *Rubber Chem. Technol.* **2004**, *76*, 13.

(27) (a) Van Gurp, M.; Palmen, J. *Rheol. Bull.* **1998**, *67*, 5. (b) Macaúbas, P. H. P.; Demarquette, N. R. *Polym. Eng. Sci.* **2002**, *42*, 1509.

(28) Wang, M. J.; Lu, S. X.; Mahmud, K. *J. Polym. Sci., Part B: Polym. Phys.* **2000**, *38*, 1240.

(29) Fesko, D. G.; Tshoegl, N. W. *J. Polym. Sci., Part C: Polym. Symp.* **1971**, *35*, 51.

(30) Gotro, J. T.; Graessley, W. W. *Macromolecules* **1984**, *17*, 2767.

(31) Tschoegl, N. W. *The Phenomenological Theory of Linear Viscoelastic Behavior*; Springer: Berlin, 1989; pp 117, 122.

(32) Dorgan, J. R.; Knauss, D. M.; Al-Muallem, H. A.; Huang, T.; Vlassopoulos, D. *Macromolecules* **2003**, *36*, 380.

(33) Gauthier, M.; Chung, J.; Choi, L.; Nguyen, T. T. *J. Phys. Chem. B* **1998**, *102*, 3138.

(34) Hempenius, M. A.; Michelberger, W.; Möller, M. *Macromolecules* **1997**, *30*, 5602.

MA0606713